

Expressing Multivariate Time Series as Graphs with Time Series Attention Transformer

William T. Ng^{3,2*}, K. Siu¹, Albert C. Cheung¹ and Michael K. Ng²

¹Radiant First Research Limited

²The University of Hong Kong

³Koi Investment Partners International Limited

william.ng@koiinvestments.com, {siu.kw, albert}@radiantfirstrresearch.com, mng@maths.hku.hk

Abstract

A reliable and efficient representation of multivariate time series is crucial in various downstream machine learning tasks. In multivariate time series forecasting, each variable depends on its historical values and there are inter-dependencies among variables as well. Models have to be designed to capture both intra and inter relationships among the time series. To move towards this goal, we propose the Time Series Attention Transformer (TSAT) for multivariate time series representation learning. Using TSAT, we represent both temporal information and inter-dependencies of multivariate time series in terms of edge-enhanced *dynamic graphs*. The intra-series correlations are represented by nodes in a dynamic graph; a self-attention mechanism is modified to capture the inter-series correlations by using the super-empirical mode decomposition (SMD) module. We applied the embedded dynamic graphs to time series forecasting problems, including two real-world datasets and two benchmark datasets. Extensive experiments show that TSAT clearly outperforms six state-of-the-art baseline methods in various forecasting horizons. We further visualize the embedded dynamic graphs to illustrate the graph representation power of TSAT. We share our code at <https://github.com/RadiantResearch/TSAT>.

1 Introduction

Multivariate time series forecasting prevails in many real-world domains, such as weather forecasting, energy output management, stock prices and exchange rate predictions. In multivariate time series modeling, it is assumed that variables not only depend on their historical values but also having to take into account the latent dependencies among the variables. For example, temperatures of a city have seasonal patterns, and additionally temperatures across neighboring cities should exhibit similar seasonality.

Time series forecasting can be divided into *univariate* and *multivariate* methods. Univariate methods analyze each time

series independently without cross-learning in the dataset. Traditional univariate methods are statistical methods. Variants of autoregressive integrated moving average (ARIMA), and exponential smoothing (ETS), are two prominent approaches. ARIMA models are popular because of their rich statistical foundations, and the Box-Jenkins methodology for its selection procedure [Hamilton, 1994]. For ETS, the Holt-Winters method [Winters, 1960; Holt, 2004] is one of the default models in the industry which uses an exponential smoothing technique for the level, trend, and seasonal components contained in the time series. In spite of the statistical interpretability of these methods, they lack adaptability and are limited when trying to capture non-linear relationships.

Multivariate methods consider multiple time series as a unified object; they naturally fit into the framework of deep learning methods due to their capability to use high dimensional data as inputs. Recurrent Neural Networks (RNN's) are designed for processing sequential data. For an example of RNN's application on multivariate time series see [Che *et al.*, 2016]. Another RNN technique, Long Short-Term Memory (LSTM) [Hochreiter and Schmidhuber, 1997], is designed to capture both the short and long-term patterns within sequential inputs and alleviate gradient vanishing and exploding problems in RNN models; for an example of LSTM on time series tasks see [Lai *et al.*, 2018; Shih *et al.*, 2019]. In spite of being able to capture non-linear patterns among time series, none of these methods explicitly considers the inter-series dependencies. Encoder-decoder attention models [Sutskever *et al.*, 2014; Chorowski *et al.*, 2014], and Transformer [Vaswani *et al.*, 2017], are alternatives to sequence-to-sequence learning. Especially, the self-attention mechanism that learns which entities in the input sequence are the most relevant to targeted values. Transformer has impressive results in natural language processing [Tay *et al.*, 2020], computer vision [Khan *et al.*, 2021], and ongoing efforts have been made to apply this method to time series tasks [Zhou *et al.*, 2021; Lim *et al.*, 2021]. Researchers have also attempted to design neural networks that use a mixture of basic architectures such as multi-layer perceptrons, RNNs, and Convolution Neural Networks (CNN's), for cross-learning on datasets. For example, LSTNet [Lai *et al.*, 2018] is composed of both CNN and RNN units; WaveNet [Oord *et al.*, 2016] uses dilated causal convolutions to capture long-term sequential depen-

*corresponding author

dencies. Yet, these methods cannot fully exploit the inter-relation among the time series, and hence the model interpretability is weakened.

Among the deep learning methods, Graph Neural Networks (GNN’s) have been successfully used to represent relationships, ranging from social network interactions, to supply chain information, to the spread of disease. A framework of graph representation learning can be summarized into three steps: 1) *Initialization step* translates the input data into a graph in terms of node features, edge features and a corresponding graph structure; 2) *Embedding step* assigns each of the graphs a unique embedding vector; 3) *Read-out step* aggregates both nodes and edge messages to represent a graph by a fixed-length output vector.

In this paper, we propose the Time Series Attention Transformer (TSAT) for multivariate time series representation learning and forecasting. First, we abstract the intra-series and inter-series correlations as a topological graph, namely *dynamic graphs*, as the temporal information is encoded and the graph structure is not static. As such, GNN can be intuitively applied to learn the representation of the dynamic graphs. Second, we attempt to integrate Transformer with GNN by augmenting the self-attention mechanism with inter-series correlation and the dynamic graph structure. The main contributions of this paper include:

- To propose the concept of an edge-enhanced dynamic graph which leads to better representation and feature engineering of multivariate time series.
- To modify the self attention mechanism for translating the time series prediction problem into graph embedding by aggregating nodes features, edges features and graph structure in one layer. Ablation studies are present to prove the effectiveness of this design.
- To provide extensive experiments on both real-world and benchmark datasets that demonstrate superior performances over the state-of-the-art methods.

The remainder of this paper is organized as follows. Section 2 lists the related work on how GNN is applied to time series forecasting. Section 3 introduces the preliminary concepts. Section 4 introduces our TSAT framework. Section 5 includes a series of experiments which we conduct and discuss. Section 6 briefly concludes the work.

2 Related work

GNN for time series forecasting. A spatial-temporal GNN assumes a physical graph structure to describe the inter-series relationships. STGCN [Yu *et al.*, 2017] assumes a traffic network and uses the graph convolutions to capture the spatial dependency among the nodes; 1D convolutions are used to model the temporal patterns. Similarly, DCRNN [Li *et al.*, 2018] uses a diffusion convolution operation and RNN units for the spatial and the temporal modelings respectively. While these methods are clearly successful, the graph structures are problem specific and require human knowledge to amend the GNNs to other problems. Another type of GNN learns the graph structures from the input time series. MT-GNN [Wu *et al.*, 2020] contains a graph learning layer which

learns a graph adjacency matrix adaptively to capture the latent relations among time series data. TEGNN [Xu *et al.*, 2020] defines causality between two nodes by transferring entropy, and hence determines the connectedness. For these methods, graph structures are learnt from the state information contained as node features without fully exploiting any edge information. There are additional mathematical tools to extract features from time series before constructing the graph structure. Time2Graph [Cheng *et al.*, 2020] and [Hu *et al.*, 2021] use shapelets to capture how time series evolve over time, and hence defines evolutionary graphs. StemGNN [Cao *et al.*, 2021] projected time series into a spectral domain by using discrete Fourier transform for capturing multivariate dependencies. In our work, the graph structure is time dependent and is decided by the outputs from our SMD module.

Transformer and GNN. There are multiple works that integrate Transformer with GNN. Graph Transformer [Dwivedi and Bresson, 2020] modifies the original transformer to adapt to a general graph topology. The attention mechanism is converted to be a function of neighborhood connectivity for each node in the graph; the sinusoidal positional encoding is replaced by graph Laplacian eigenvectors. Graph Transformer Network (GTN) [Yun *et al.*, 2019] uses the attention mechanism to determine how to generate a meta-path between two nodes in a heterogeneous graph. A spatio-temporal GTN [Yu *et al.*, 2020] adopted graph convolution to incorporate spatial information into Transformer, allowing the model to predict a pedestrian trajectory. Molecular Attention Transformer [Maziarka *et al.*, 2020] augments the attention mechanism with inter-molecular distances and structures. Inspired by methods augmenting the self-attention mechanism with domain specific knowledge, our model encourages to improve the self-attention to adapt the node features, edge features and the graph structure of dynamic graphs.

3 Preliminaries

In this section, we present a novel representation learning algorithm for time series modeling. We extract features of each time series by means of super-empirical mode decomposition. The extracted feature is a set of intrinsic mode functions (IMFs) which can be expressed analytically using cosine polynomials with time-varying frequencies. We shall define a dynamic graph in terms of IMFs and incorporate the IMFs into a multi-head self-attention mechanism for learning inter-series relations.

Super-empirical mode decomposition. A super-empirical mode decomposition (SMD) [Chui *et al.*, 2016] is a time-analysis scheme to decompose an input time series into a finite sum of *intrinsic mode functions* (IMFs) f_i . i.e., given a time series $x(t)$, the SMD scheme gives

$$x(t) = \sum_{i=1}^K f_i(t) + R(t) \quad (1)$$

$$f_i(t) = A_i(t) \cos(2\pi\phi_i(t)). \quad (2)$$

Here, $\phi_i(t)$ refers to a non-stationary phase function and its derivative $\phi_i'(t)$ is the instantaneous frequency; $A_i(t)$ is the

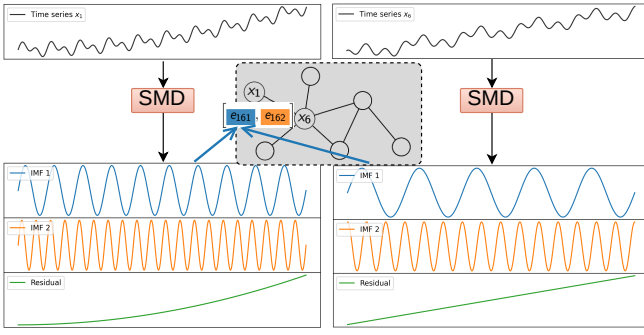


Figure 1: Each series is decomposed by SMD into a set of IMFs with a residual representing its trend. Series with similar trends are connected by an edge. Edge features are calculated by pairwise IMFs.

instantaneous amplitude; $R(t)$ is a residual term which indicates a trend of the time series. In TSAT, we make use of SMD as a feature extraction module. The IMFs are key features extracted from input time series. We choose SMD over discrete Fourier transforms because the frequency contents in real-life signals are time varying.

Problem definition and dynamic graphs. In multivariate time series forecasting of a rolling manner, we consider fixed lengths of backcast L_x and forecast L_y . At time t , the input $\mathcal{X}^t = \{\mathbf{x}_1^t, \dots, \mathbf{x}_{L_x}^t \mid \mathbf{x}_i^t \in \mathbb{R}^N\}$ is a set of N time series of observed values and it aims to predict future values in a set $\mathcal{Y}^t = \{\mathbf{y}_1^t, \dots, \mathbf{y}_{L_y}^t \mid \mathbf{y}_i^t \in \mathbb{R}^N\}$. Then, a dynamic graph G^t is defined as a triple $(\mathbf{X}^t, \mathcal{E}^t, \mathbf{A}^t)$, where $\mathbf{X}^t \in \mathbb{R}^{N \times L_x}$ is a *node matrix* whose columns are formed sequentially from the set \mathcal{X}^t . Each of the nodes contains L_x historical values for each time series. $\mathcal{E}^t = (e_{ijk}) \in \mathbb{R}^{N \times N \times K}$ is an *edge tensor* in which e_{ijk} represents a correlation of the k^{th} IMFs $f_{\cdot,k}$ between time series x_i and x_j given by

$$\frac{f_{i,k}^T f_{j,k}}{\|f_{i,k}\|_2 \|f_{j,k}\|_2}. \quad (3)$$

See Figure 1. Lastly, we emphasize that the graph structure is time-dependent and learnt from the input data. We use $\mathbf{A}^t \in \mathbb{R}^{N \times N}$, where $a_{ij} \in \{0, 1\}$ denotes the connectedness among the nodes. We compute the correlation of residuals of time series x_i and x_j by

$$\rho_{ij} = \frac{R_i^T R_j}{\|R_i\|_2 \|R_j\|_2}. \quad (4)$$

Then, the \mathbf{A}^t is defined by

$$a_{ij}^t = \begin{cases} 1 & \text{if } |\rho_{ij}| > c \\ 0 & \text{otherwise.} \end{cases}$$

i.e., from SMD, the residual of a time series determines its trend. Thus, we define an edge between two nodes if their trends are highly correlated with a threshold value c . As such, the multivariate time series forecasting problem is formulated as a node-level supervised learning problem with additional information contained in edges.

$$\mathbf{Y}^t = F(G^t; \Theta), \quad (5)$$

where F is a forecasting model with parameters Θ , and \mathbf{Y}^t is formed by stacking entries from the set \mathcal{Y}^T . As dynamic graphs cover a wide range of possible situations of multiple time series, they need a flexible model for graph learning tasks. Our contribution is designing a modified transformer model to represent the dynamic graphs effectively.

Attention mechanism. The original Transformer has M attention blocks. In each block there is a multi-head self-attention layer, followed by a residual connection, and a Layer Normalization [Ba *et al.*, 2016] to enhance the scalability of the model. The multi-head self-attention has H heads. Denote the input matrix $\mathbf{H} \in \mathbb{R}^{n \times d}$ where n and d are the length and dimension of the input sequence. In each head i ($i = 1, \dots, H$), the operation is composed of two parts. 1) A *transformation layer* projects X to three sequential matrices, namely queries, key and values respectively by

$$\mathbf{Q}_i = \mathbf{H}\mathbf{W}^{Q_i}, \mathbf{K}_i = \mathbf{H}\mathbf{W}^{K_i}, \mathbf{V}_i = \mathbf{H}\mathbf{W}^{V_i}, \quad (6)$$

where $\mathbf{W}^{Q_i} \in \mathbb{R}^{d \times d_k}$, $\mathbf{W}^{K_i} \in \mathbb{R}^{d \times d_k}$ and $\mathbf{W}^{V_i} \in \mathbb{R}^{d \times d_v}$ are three learnable weight matrices. 2) An *attention layer* computes the ‘‘attention’’ among the queries and keys and assigns the scores to values. The output of each of the i attention operations is given by

$$\mathcal{A}_i = \sigma \left(\frac{\mathbf{Q}_i \mathbf{K}_i^T}{\sqrt{d_k}} \right) \mathbf{V}_i, \quad (7)$$

where σ is the softmax function and the scaling factor $\sqrt{d_k}$ is present in case of gradient vanishing. All the H outputs are concatenated into a single matrix $[\mathcal{A}_1, \dots, \mathcal{A}_H] \in \mathbb{R}^{n \times H \cdot d_v}$ and then mapped by an output weight matrix $\mathbf{W}^O \in \mathbb{R}^{H \cdot d_v \times d}$.

4 The framework of TSAT

In this section, we describe the architecture (Figure 2) of the Time Series Attention Transformer (TSAT). Especially, we discuss how the original self-attention mechanism is modified to capture the characteristics of time series.

Time embedding layer. In an ordinary Transformer, the attention mechanism neglects the order of elements in a sequence because the mechanism treats each input element simultaneously and identically. To incorporate the sequential information, a positional vector is added to each of the elements in the input sequence. Recall that the inputs of TSAT are dynamic graphs which explicitly contain temporal information. We adopt a RNN layer [Liu *et al.*, 2020] as a position embedding layer on the node matrix \mathbf{X}^t which contains temporal information as

$$h(\mathbf{X}^t) = \text{RNN}(\mathbf{X}^t) \quad (8)$$

before further passing the hidden features $h(\mathbf{X}^t)$ to the next layer.

Time series self-attention. The original Transformer model is designed for sequence-to-sequence learning. We do not consider the dynamic graphs as sentences to be encoded. This would require additional handcrafted representations to

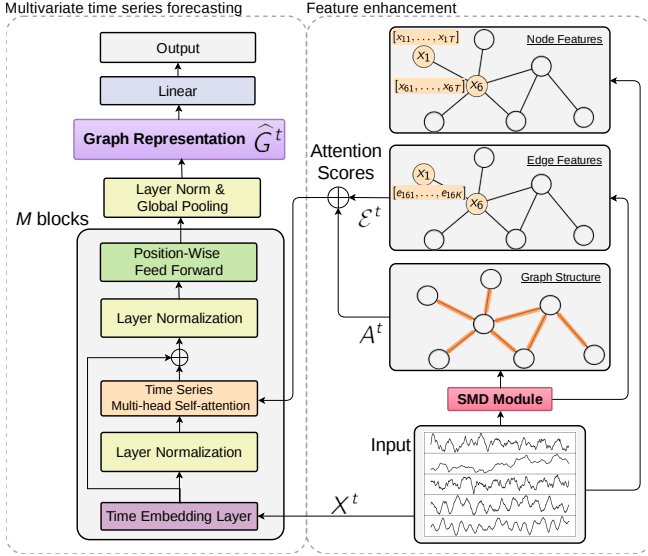


Figure 2: TSAT. The multi-head self-attention computes attention scores of three main components of a dynamic graphs, namely node features, edge features and the graph structure.

treat dynamic graphs as strings. Instead, to aggregate information of nodes, edges and the graph structure, the multi-head self-attention operation (7) is modified as

$$\mathcal{A}_i = \left(\alpha_0 \sigma \left(\frac{\mathbf{Q}_i \mathbf{K}_i^T}{\sqrt{d_k}} \right) + \sum_{k=1}^K \alpha_k \sigma(\mathbf{D}_{\text{imf}_k}) + \alpha_{K+1} \mathbf{A} \right) \mathbf{V}_i, \quad (9)$$

where $\alpha_i (i = 0, \dots, K + 1)$ are trainable parameters with respect to these three pieces of information: 1) *Node features*. The first term $\mathbf{Q}_i \mathbf{K}_i^T / \sqrt{d_k}$ is an original self-attention layer which takes care of the intra-time series relation contained in nodes directly. 2) *Edge features*. There are K terms for inter-series relation. $\mathbf{D}_{\text{imf}_k}$ is a covariance matrix of the k^{th} IMF of all time series. 3) *Adjacency matrix*. The last term \mathbf{A} is an adjacency matrix of the dynamic graph. In a word, the TSAT operation (9) is designed for a holistic representation of a dynamic graph. It captures the node, edge, and adjacency information simultaneously in one layer.

Time series transformer and the read-out. The output of TSAT layers are followed by another Layer Normalization and a position-wise Feed Forward Network (FFN) as the original Transformer encoder does. This is one block of a time series attention transformer. The TSAT block is repeated M times; another Layer Normalization and a global average pooling layer are added for regularization, giving our a set of embedded dynamic graphs \hat{G}^t . A fully connected layer $f(\cdot)$ is used for downstream machine learning tasks by setting $\mathbf{Y}^t = f(\hat{G}^t)$.

5 Experiments

In this section, we evaluate TSAT on multivariate time series forecasting. To have a standardized comparison to other baseline methods, we adopt a similar setting to Informer [Zhou *et al.*, 2021]. We address three research questions:

Dataset	# samples	# nodes	sample rate
ETTh ₁	17420	7	hourly
ETTh ₂	17420	7	hourly
ETTm ₁	69600	7	15-minute
Weather	35064	1600	hourly
Electricity	26304	321	hourly

Table 1: Dataset statistics.

- How does TSAT perform compared with state-of-the-art time series forecasting models?
- Does the formulation of dynamic graphs with nodes, edge features and the graph structure lead to better results?
- Is TSAT effective in graph representation learning for multivariate time series?

5.1 Experimental settings

Benchmark datasets

There are four datasets and five cases, including two real-world datasets and two public benchmark datasets.

ETT (Electricity transformer temperature). This is the same dataset as used by Informer¹. The two-year data are recorded in two different provinces (each of seven regions) in China. The dataset is resampled as two hourly datasets, namely ETTh₁ and ETTh₂; and a fifteen-minute dataset, namely ETTm₁. The target value is “oil temperature”.

Weather. This dataset was obtained from National Centers for Environmental Information². It contains 1600 locations of hourly data from 2018 to 2020 in the United States. The dataset contains eleven climate features such as visibility, dew point temperature, humidity, etc. The target value is the “web-bulb” temperature.

Electricity. This dataset is collected from UCI machine learning repository³ which contains hourly electricity consumption of 321 clients over two years.

All the datasets are split into 80% training data and 20% as testing data in a sequential manner. Among the training datasets, the last 10% is reserved as a validation set for the model early stopping. Detailed statistics are found in Table 1.

Implementation details

Baseline models. We selected a comprehensive set of six baseline methods composed of three categories to test against TSAT. (1) *Statistical*: ARIMA [Contreras *et al.*, 2003] is a traditional statistical model, and DeepAR [Salinas *et al.*, 2020] is a deep learning-based autoregressive model. (2) *Deep Learning*: Informer is a sparse attention based model, and LSTNet [Lai *et al.*, 2018] is composed of both CNN and RNN units. (3) *GNN based*. MTGNN [Wu *et al.*, 2020] is a graph convolutional model, and Graph WaveNet [Wu *et al.*, 2019] is a spatial-temporal graph convolution model with 1D convolution units.

¹<https://github.com/zhouhaoyi/ETDataset>

²<https://www.ncei.noaa.gov/data/local-climatological-data/>

³<https://archive.ics.uci.edu/ml/datasets/ElectricityLoadDiagrams20112014>

Hyper-parameter tuning. For each method, we conduct a grid search for tuning hyper-parameters. The hyper-parameter range can be found in the Appendix. Especially, to illustrate the representation power of TSAT, the embedding dimension was chosen by $d_k = \lfloor L_x/2^n \rfloor$ for $n \in \{1, 2, 3, 4\}$. We adopt ADAM as a stochastic optimization model with a batch size equal to 64. An initial learning rate is $1e^{-4}$ and it decays exponentially with parameter $5e^{-3}$ on each epoch.

Metrics of comparison. For hourly datasets, the forecast horizon $L_y = \{24, 48, 168, 336, 720\}$; for the dataset of every fifteen minutes, $L_y = \{24, 48, 168, 336, 720\}$. For the input backcast length, we choose $L_x = m \times L_y (m = 1, 2, 3, 4)$. The following two evaluation metrics are used: $RMSE = \sqrt{1/n \sum_{i=1}^N (\mathbf{y} - \hat{\mathbf{y}})^2}$ and $MAE = 1/n \sum_{i=1}^N |\mathbf{y} - \hat{\mathbf{y}}|$. To evaluate performance across the datasets, metrics are computed on the normalized samples.

5.2 Performance comparison

The complete results of each model on all datasets are displayed in Table 2 in which the best previous methods are underlined, and the best overall methods are shown with bold style. From the results, we observe that: (1) The proposed model TSAT has significant improvements on all datasets of different forecast horizons. TSAT records improvements in 30 out of 46 cases. For winners of each category, TSAT has better results for average RMSE than MTGNN, LSTNet and DeepAR, by 8.02%, 16.01% and 48.28% respectively, when compared to the real world datasets $\{ETTh_1, ETTh_2, ETTm_1\}$. In the open benchmark dataset $\{\text{Weather}, \text{Electricity}\}$, the improvement in average RMSE is 6.7%, 23.66% and 50.04% over the same set of baseline methods. (2) TSAT performs better than a degraded version of TSAT, taking away both edge features and adjacency information of a dynamic graph. This indicates that both features are helpful to achieve more accurate results. (3) In two benchmark datasets $\{\text{Weather}, \text{Electricity}\}$ composed of a large number of multivariate time series (nodes), for example Electricity which has 321 time series, both TSAT and the GNN based models show superior results over the deep learning methods, and the univariate statistical methods. TSAT, MTGNN and Graph WaveNet improved by 14.66%, 13.80% and 13.47% for average RMSE on benchmark datasets, compared to real world datasets. This confirms that the graph structure can enhance the performance of tasks performed on large datasets.

5.3 Ablation studies

To better understand how edge features and adjacency contribute to TSAT, we include a series of ablation studies in Table 3. TSAT achieved the best results (4 out of 5 counts) when both edges and the adjacency were used as inputs. When either the edge feature or the graph structure was omitted, the performance was slightly worse than TSAT, by -1.65% and -0.57%. TSAT without both edge features and graph structure gave the worst performance. We conclude that both the use of edges features and the graph structure are essential in the performance of TSAT.

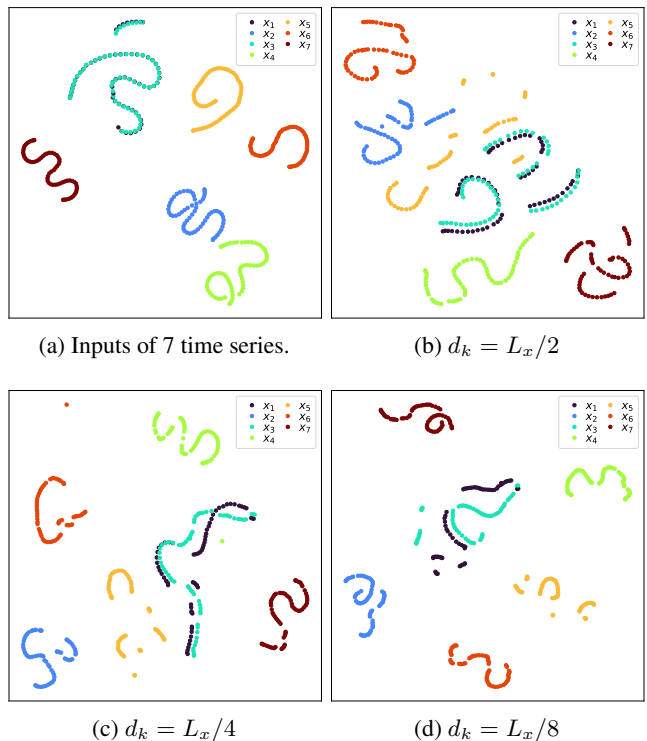


Figure 3: (a) t-SNE plots of the inputs. (b), (c) and (d) Embedded graphs of different embedding dimensions.

5.4 Visualization of embedded dynamic graphs

To illustrate the information preserved after using TSAT, we adopt t-distributed stochastic neighbor embedding (t-SNE) to visualize the embedded dynamic graphs of the dataset $ETTh_1$. Figure 3(a) shows a t-SNE plot composed of seven time series with length $L_x = 720$. There are clearly six clusters of points, however we observe that time series x_1 and x_4 almost overlap to each other, reflecting the similarity between these two time series in the original real world data. Figures 3(b), (c) and (d) show the t-SNE plots of TSAT outputs of different embedding dimensions ($d_k = 90, 180$ and 360). With the additional edge features and the graph structure used by TSAT, the time series x_1 and x_4 become distinguishable. This result suggests that TSAT captures better representations of a set of multiple time series.

6 Conclusions

In this paper, we propose a Time Series Attention Transformer (TSAT) to translate a time series embedding problem into a graph representation problem. In the edge-enhanced dynamic graph, the inter-correlations of time series are strengthened by correlations of corresponding intrinsic mode functions which capture different cycles hidden in the input time series. The self-attention mechanism is augmented to capture a tuple of information from a graph. Extensive experiments demonstrate that our TSAT displays superior performance when compared with state-of-the-art baselines over both the real world datasets and the benchmark datasets.

Type	Proposed model				GNN based				Deep learning				Statistical				
Method	TSAT		TSAT w/o graph		MTGNN		Graph WaveNet		Informer		LSTNet		DeepAR		ARIMA		
Metric	RMSE	MAE	RMSE	MAE	RMSE	MAE	RMSE	MAE	RMSE	MAE	RMSE	MAE	RMSE	MAE	RMSE	MAE	
ETTh ₁	24	0.1864	0.1424	0.1940	0.1491	<u>0.2002</u>	<u>0.1529</u>	0.2038	0.1569	0.4828	0.4101	0.2334	0.1845	0.4940	0.4397	0.2039	0.1553
	48	0.1964	0.1508	0.2065	0.1594	0.2135	0.1656	0.2189	0.1682	0.4978	0.4160	0.2205	0.1833	0.4767	0.4242	<u>0.2101</u>	<u>0.1627</u>
	168	0.2283	0.1773	0.2341	0.1832	0.2505	0.1965	0.2544	0.1970	0.4861	0.4021	0.2241	0.1908	0.4662	0.4132	0.2226	0.1735
	336	0.2391	0.1866	0.2402	0.1886	0.2569	0.2002	0.2632	0.2023	0.5198	0.4373	0.2626	0.2118	0.4564	0.4064	0.2307	0.1791
	720	0.2492	0.1941	0.2519	0.1960	0.2687	0.2066	0.2746	0.2111	0.3176	0.2522	0.3254	0.2598	0.4911	0.4388	0.2432	0.1877
ETTh ₂	24	0.2256	0.1788	0.2329	0.1837	<u>0.2427</u>	<u>0.1910</u>	0.2456	0.1941	0.2942	0.2247	0.2881	0.2205	0.5251	0.4786	0.3085	0.2206
	48	0.2310	0.1810	0.2391	0.1885	0.2455	0.1938	0.2509	0.1966	0.3552	0.2757	<u>0.2399</u>	<u>0.1886</u>	0.4895	0.4420	0.4029	0.2671
	168	0.2628	0.2073	0.2578	0.2032	<u>0.2953</u>	<u>0.2334</u>	0.3002	0.2361	0.5266	0.4224	0.5254	0.3321	0.5097	0.4645	0.4254	0.4144
	336	0.2858	0.2251	0.2907	0.2308	0.3238	0.2534	0.3274	0.2565	0.5203	0.4197	<u>0.3102</u>	<u>0.2482</u>	0.5056	0.4599	3.0331	3.4774
	720	0.3205	0.2522	0.3109	0.2471	<u>0.3453</u>	<u>0.2696</u>	0.3485	0.2745	0.5259	0.4281	0.5929	0.5288	0.4998	0.4423	2.4774	2.2194
ETTm ₁	24	0.2159	0.1710	0.2177	0.1735	<u>0.2321</u>	<u>0.1831</u>	0.2344	0.1858	0.3341	0.2914	0.2714	0.2220	0.5661	0.5214	5.4671	4.0550
	48	0.2386	0.1839	0.2396	0.1843	<u>0.2554</u>	<u>0.1977</u>	0.2585	0.1995	0.4561	0.4025	0.2820	0.2283	0.5310	0.4889	5.1506	3.8408
	168	0.3015	0.2262	0.2983	0.2242	<u>0.3228</u>	<u>0.2433</u>	0.3265	0.2461	0.5764	0.4990	0.3049	0.2443	0.5158	0.4665	4.6019	3.4607
	336	0.3467	0.2600	0.3476	0.2607	0.3714	0.2782	0.3757	0.2842	0.5766	0.4939	0.3213	0.2562	0.4962	0.4469	4.4510	3.3483
	720	0.3703	0.2782	0.3658	0.2730	0.4141	0.3132	0.4276	0.3217	0.6845	0.6068	0.3393	0.2731	0.5133	0.4698	4.4076	3.2886
Weather	48	0.2045	0.1566	0.2177	0.1687	0.2313	0.1802	0.2428	0.1854	0.5826	0.4947	0.4181	0.4649	0.5400	0.4853	<u>0.2234</u>	<u>0.1596</u>
	168	0.2473	0.1898	0.2593	0.2001	<u>0.2716</u>	<u>0.2099</u>	0.2806	0.2157	0.6756	0.5713	0.4599	0.4982	0.5415	0.4817	0.2897	<u>0.2066</u>
	336	0.2674	0.2046	0.2765	0.2113	<u>0.2925</u>	<u>0.2234</u>	0.2969	0.2266	0.7177	0.6180	0.4948	0.4250	0.5191	0.4587	0.9631	0.3099
	720	0.2903	0.2222	0.2943	0.2253	<u>0.3139</u>	<u>0.2396</u>	0.3197	0.2426	0.7075	0.6044	0.4513	0.4764	0.5357	0.4726	0.8007	1.0085
	Electricity	12	0.1743	0.1209	0.1794	0.1248	<u>0.1887</u>	<u>0.1304</u>	0.1907	0.1322	0.6314	0.5057	0.3484	0.3585	0.5089	0.4700	0.4182
	24	0.1842	0.1258	0.1895	0.1303	<u>0.1972</u>	<u>0.1344</u>	0.1997	0.1369	0.5603	0.4550	0.3025	0.3615	0.5044	0.4653	0.4590	0.4608
	48	0.1982	0.1332	0.2001	0.1352	<u>0.2146</u>	<u>0.1437</u>	0.2171	0.1479	0.6331	0.5333	0.3001	0.3590	0.5054	0.4654	0.5522	0.5693
	72	0.2066	0.1361	0.2086	0.1383	<u>0.2387</u>	<u>0.1562</u>	0.2416	0.1578	0.6334	0.5981	0.3539	0.4071	0.5059	0.4668	0.5903	0.5778
Count	30		6		0		0		0		4		0		6		

Table 2: Prediction results of TSTAT and 6 baselines of 3 categories on 5 cases.

Method	ETTh ₁	ETTh ₂	ETTm ₁	Weather	Electricity
TSAT w/o graph	0.2253	0.2663	0.2938	0.2620	0.1944
TSAT w/o edge	0.2208	0.2648	0.2967	0.2528	0.1910
TSAT w/o adj	0.2237	0.2673	0.2946	0.2595	0.1945
TSAT	0.2198	0.2651	0.2906	0.2524	0.1908

Table 3: Ablation results on 5 datasets (measured in average RMSE over different forecast horizons).

References

- [Ba *et al.*, 2016] Jimmy Lei Ba, Jamie Ryan Kiros, and Geoffrey E Hinton. Layer normalization. *arXiv preprint arXiv:1607.06450*, 2016.
- [Cao *et al.*, 2021] Defu Cao, Yujing Wang, Juanyong Duan, Ce Zhang, Xia Zhu, Conguri Huang, Yunhai Tong, Bixiong Xu, Jing Bai, Jie Tong, et al. Spectral temporal graph neural network for multivariate time-series forecasting. *arXiv preprint arXiv:2103.07719*, 2021.
- [Che *et al.*, 2016] Zhengping Che, Sanjay Purushotham, Kyunghyun Cho, David A. Sontag, and Yan Liu. Recurrent neural networks for multivariate time series with missing values. *CoRR*, abs/1606.01865, 2016.
- [Cheng *et al.*, 2020] Ziqiang Cheng, Yang Yang, Wei Wang, Wenjie Hu, Yueting Zhuang, and Guojie Song. Time2graph: Revisiting time series modeling with dynamic shapelets. In *Proceedings of the AAAI Conference on Artificial Intelligence*, volume 34, pages 3617–3624, 2020.
- [Chorowski *et al.*, 2014] Jan Chorowski, Dzmitry Bahdanau, Kyunghyun Cho, and Yoshua Bengio. End-to-end continuous speech recognition using attention-based recurrent nn: First results. *arXiv preprint arXiv:1412.1602*, 2014.
- [Chui *et al.*, 2016] Charles K Chui, HN Mhaskar, and Maria D van der Walt. Data-driven atomic decomposition via frequency extraction of intrinsic mode functions. *GEM-International Journal on Geomathematics*, 7(1):117–146, 2016.
- [Contreras *et al.*, 2003] Javier Contreras, Rosario Espinola, Francisco J Nogales, and Antonio J Conejo. Arima models to predict next-day electricity prices. *IEEE transactions on power systems*, 18(3):1014–1020, 2003.
- [Dwivedi and Bresson, 2020] Vijay Prakash Dwivedi and Xavier Bresson. A generalization of transformer networks to graphs. *CoRR*, abs/2012.09699, 2020.
- [Hamilton, 1994] James Hamilton. D.(1994), time series analysis. *Princeton, New Jersey: Princeton University Press*, 10:9780691218632, 1994.
- [Hochreiter and Schmidhuber, 1997] Sepp Hochreiter and Jürgen Schmidhuber. Long short-term memory. *Neural computation*, 9(8):1735–1780, 1997.
- [Holt, 2004] Charles C Holt. Forecasting seasonals and trends by exponentially weighted moving averages. *International journal of forecasting*, 20(1):5–10, 2004.
- [Hu *et al.*, 2021] Wenjie Hu, Yang Yang, Ziqiang Cheng, Carl Yang, and Xiang Ren. Time-series event prediction with evolutionary state graph. In Liane Lewin-Eytan,

- David Carmel, Elad Yom-Tov, Eugene Agichtein, and Evgeniy Gabrilovich, editors, *WSDM '21, The Fourteenth ACM International Conference on Web Search and Data Mining, Virtual Event, Israel, March 8-12, 2021*, pages 580–588. ACM, 2021.
- [Khan *et al.*, 2021] Salman Khan, Muzammal Naseer, Munawar Hayat, Syed Waqas Zamir, Fahad Shahbaz Khan, and Mubarak Shah. Transformers in vision: A survey. *arXiv preprint arXiv:2101.01169*, 2021.
- [Lai *et al.*, 2018] Guokun Lai, Wei-Cheng Chang, Yiming Yang, and Hanxiao Liu. Modeling long-and short-term temporal patterns with deep neural networks. In *The 41st International ACM SIGIR Conference on Research & Development in Information Retrieval*, pages 95–104, 2018.
- [Li *et al.*, 2018] Yaguang Li, Rose Yu, Cyrus Shahabi, and Yan Liu. Diffusion convolutional recurrent neural network: Data-driven traffic forecasting. In *6th International Conference on Learning Representations, ICLR 2018, Vancouver, BC, Canada, April 30 - May 3, 2018, Conference Track Proceedings*. OpenReview.net, 2018.
- [Lim *et al.*, 2021] Bryan Lim, Sercan Ö Arık, Nicolas Loeff, and Tomas Pfister. Temporal fusion transformers for interpretable multi-horizon time series forecasting. *International Journal of Forecasting*, 2021.
- [Liu *et al.*, 2020] Xuanqing Liu, Hsiang-Fu Yu, Inderjit Dhillon, and Cho-Jui Hsieh. Learning to encode position for transformer with continuous dynamical model. In *International Conference on Machine Learning*, pages 6327–6335. PMLR, 2020.
- [Maziarka *et al.*, 2020] Lukasz Maziarka, Tomasz Danel, Slawomir Mucha, Krzysztof Rataj, Jacek Tabor, and Stanislaw Jastrzebski. Molecule attention transformer. *CoRR*, abs/2002.08264, 2020.
- [Oord *et al.*, 2016] Aaron van den Oord, Sander Dieleman, Heiga Zen, Karen Simonyan, Oriol Vinyals, Alex Graves, Nal Kalchbrenner, Andrew Senior, and Koray Kavukcuoglu. Wavenet: A generative model for raw audio. *arXiv preprint arXiv:1609.03499*, 2016.
- [Salinas *et al.*, 2020] David Salinas, Valentin Flunkert, Jan Gasthaus, and Tim Januschowski. Deepar: Probabilistic forecasting with autoregressive recurrent networks. *International Journal of Forecasting*, 36(3):1181–1191, 2020.
- [Shih *et al.*, 2019] Shun-Yao Shih, Fan-Keng Sun, and Hung-yi Lee. Temporal pattern attention for multivariate time series forecasting. *Machine Learning*, 108(8):1421–1441, 2019.
- [Sutskever *et al.*, 2014] Ilya Sutskever, Oriol Vinyals, and Quoc V Le. Sequence to sequence learning with neural networks. In *Advances in neural information processing systems*, pages 3104–3112, 2014.
- [Tay *et al.*, 2020] Yi Tay, Mostafa Dehghani, Dara Bahri, and Donald Metzler. Efficient transformers: A survey. *arXiv preprint arXiv:2009.06732*, 2020.
- [Vaswani *et al.*, 2017] Ashish Vaswani, Noam Shazeer, Niki Parmar, Jakob Uszkoreit, Llion Jones, Aidan N Gomez, Łukasz Kaiser, and Illia Polosukhin. Attention is all you need. In *Advances in neural information processing systems*, pages 5998–6008, 2017.
- [Winters, 1960] Peter R Winters. Forecasting sales by exponentially weighted moving averages. *Management science*, 6(3):324–342, 1960.
- [Wu *et al.*, 2019] Zonghan Wu, Shirui Pan, Guodong Long, Jing Jiang, and Chengqi Zhang. Graph wavenet for deep spatial-temporal graph modeling. *arXiv preprint arXiv:1906.00121*, 2019.
- [Wu *et al.*, 2020] Zonghan Wu, Shirui Pan, Guodong Long, Jing Jiang, Xiaojun Chang, and Chengqi Zhang. Connecting the dots: Multivariate time series forecasting with graph neural networks. In *Proceedings of the 26th ACM SIGKDD International Conference on Knowledge Discovery & Data Mining*, pages 753–763, 2020.
- [Xu *et al.*, 2020] Haoyan Xu, Yida Huang, Ziheng Duan, Jie Feng, and Pengyu Song. Multivariate time series forecasting based on causal inference with transfer entropy and graph neural network. *CoRR*, abs/2005.01185, 2020.
- [Yu *et al.*, 2017] Bing Yu, Haoteng Yin, and Zhanxing Zhu. Spatio-temporal graph convolutional neural network: A deep learning framework for traffic forecasting. *CoRR*, abs/1709.04875, 2017.
- [Yu *et al.*, 2020] Cunjun Yu, Xiao Ma, Jiawei Ren, Haiyu Zhao, and Shuai Yi. Spatio-temporal graph transformer networks for pedestrian trajectory prediction. In *European Conference on Computer Vision*, pages 507–523. Springer, 2020.
- [Yun *et al.*, 2019] Seongjun Yun, Minbyul Jeong, Raehyun Kim, Jaewoo Kang, and Hyunwoo J Kim. Graph transformer networks. *Advances in Neural Information Processing Systems*, 32:11983–11993, 2019.
- [Zhou *et al.*, 2021] Haoyi Zhou, Shanghang Zhang, Jieqi Peng, Shuai Zhang, Jianxin Li, Hui Xiong, and Wancai Zhang. Informer: Beyond efficient transformer for long sequence time-series forecasting. In *Thirty-Fifth AAAI Conference on Artificial Intelligence, AAAI 2021, Thirty-Third Conference on Innovative Applications of Artificial Intelligence, IAAI 2021, The Eleventh Symposium on Educational Advances in Artificial Intelligence, EAAI 2021, Virtual Event, February 2-9, 2021*, pages 11106–11115. AAAI Press, 2021.

Technical appendix

Hyperparameter ranges

For reproductivity of the experiments, hyperparameter ranges used in training are listed for each model.

Time series attention Transformer. Table 4 shows hyperparameter ranges used for TSAT. Here is a list of descriptions of each parameter:

- EDGE DIM - number of IMFs used for edge features for the SMD module
- EMBED DIM - embedding dimension of the backcast horizon of time series
- ACT FUN IMF - activation function used for entries in covariance matrices of IMFs (see Equation 9)
- TSAT BLOCK - number of TSAT block repeated (M used in Figure 2)
- LAYER OUTPUT - number of fully connected layers used for machine learning tasks
- ACT FUN OUTPUT - activation function that used in the LAYER OUTPUT
- DROPOUT - dropout is used between each TSAT block and the final output fully connected layer

Table 4: TSAT hyperparameter ranges.

Item	Parameter
BATCH SIZE	8, 16, 32, 64
LEARNING RATE	1e-4, decaying with 5e-3
MAX EPOCH	2000 with early stopping
EDGE DIM	3, 4, 5
EMBED DIM	45, 90, 180, 256, 360
TSAT BLOCK	1, 2, 4, 8
ATTENTION HEAD	4, 8, 16
LAYER OUTPUT	1, 2, 4
ACT FUN OUTPUT	ReLU
ACT FUN IMF	'exp', 'softmax', 'none'
DROPOUT	0.1, 0.2

GNN based models. MTGNN⁴ and Graph WaveNet⁵ are used as baseline GNN methods. Hyperparameter ranges for these methods are listed in Tables 5 and 6. For both methods, we basically followed the suggested experimental setup and provided additional parameter choices for some items to adapt to our datasets.

⁴<https://github.com/nanzhan/MTGNN>

⁵<https://github.com/nanzhan/Graph-WaveNet>

Table 5: MTGNN hyperparameter ranges.

Item	Parameter
BATCH SIZE	16, 32, 64
LEARNING RATE	0.001, 0.0015, 0.002
EPOCHS	100, 200, 300
l_2 REGULARIZATION	0.0001, 0.00015, 0.0002
DROPOUT	0.1, 0.2, 0.3
GRAPH LEARNING LAYER	2, 3
MIX-HOP PRO LAYER	2
NUM SPLIT	1,2,3
NODE EMBED	40

Table 6: Graph WaveNet hyperparameter ranges.

Item	Parameter
BATCH SIZE	16, 32, 64
LEARNING RATE	0.001, 0.002, 0.003
WEIGHT DECAY	0.0001, 0.0005, 0.001
EPOCH	100, 150, 200
INPUT LEN	72, 168, 720
RANDOMADJ	True, False
NUM HID LAYER	32, 64
MODEL DROPOUT	0.1, 0.2, 0.3

Deep learning models. Informer⁶ and LSTNet⁷ are used as baseline methods of deep learning. Their hyperparameter ranges are included in Tables 7 and 8.

Table 7: Informer hyperparameter ranges.

Item	Parameter
BATCH SIZE	16, 32
LEARNING RATE	0.0001, 0.005, 0.01
EPOCH	20, 30
INPUT SEQUENCE LEN	168, 720
ENCODER INPUT	7
DECODER INPUT	7
MODEL DROPOUT	0, 0.05
EXPERIMENT REPEAT	2

Table 8: LSTNet hyperparameter ranges.

Item	Parameter
CONV1 OUT CHANNELS	32, 64
CONV1 KERNEL HEIGHT	7
RECC1 OUT CHANNELS	32, 64
SKIP STEPS	4, 12, 24
SKIP RECCS OUT CHANNELS	2, 4, 6
AR WINDOW SIZE	7
MODEL DROPOUT	0.2

⁶<https://github.com/zhouhaoyi/Informer2020>

⁷<https://github.com/laiguokun/LSTNet>

Statistical models. DeepAR and ARIMA are used as baseline statistical methods. Their hyperparameter ranges are listed in Tables 9 and 10. For DeepAR, we adopted the default settings with the Electricity dataset while we included some more parameters for the grid search.

Table 9: DeepAR hyperparameter ranges.

Item	Parameter
BATCH SIZE	32, 64
LEARNING RATE	0.0001, 0.005, 0.01
ENCODER	32, 64, 168
INPUT EMBED	120, 370
OUTPUT EMBED	20, 40
LSTM LAYER	2, 3
LSTM NODES	20, 40

Table 10: ARIMA hyperparameter ranges.

Item	Parameter
DIFFERENCING (d)	0, 1
MOV AVG WINDOW (q)	0, 5, 10